

NATIONAL ADVISORY COMMITTEE FOR AERONAUTICS

TECHNICAL NOTE 4255

WIND-TUNNEL INVESTIGATION AT LOW SPEEDS OF FLIGHT
CHARACTERISTICS OF A SWEEPBACK-WING JET-TRANSPORT
AIRPLANE MODEL EQUIPPED WITH AN EXTERNAL-FLOW
JET-AUGMENTED SLOTTED FLAP

By Joseph L. Johnson, Jr.

Langley Aeronautical Laboratory
Langley Field, Va.



Washington

July 1958

AFMCG

TECHNICAL LIBRARY
APR 2011



TECHNICAL NOTE 4255

WIND-TUNNEL INVESTIGATION AT LOW SPEEDS OF FLIGHT
CHARACTERISTICS OF A SWEEPBACK-WING JET-TRANSPORT
AIRPLANE MODEL EQUIPPED WITH AN EXTERNAL-FLOW
JET-AUGMENTED SLOTTED FLAP

By Joseph L. Johnson, Jr.

SUMMARY

A wind-tunnel investigation at low speeds has been made to determine the flight characteristics of a model of a sweptback-wing jet-transport airplane equipped with an external-flow jet-augmented slotted flap. The model was flown in the flap-retracted configuration over a lift-coefficient range from 0.6 to 0.9 and in the flap-extended configuration over a lift-coefficient range up to about 12.5 for a range of angles of attack from -12° to about 13° . For tests at the very high lift coefficients, a downwardly directed nose jet was used to supplement the trimming power of the horizontal tail.

The model was flown up to a lift coefficient of 6 without the nose jet, but the longitudinal stability was considered satisfactory only at lift coefficients below about 4. The use of the nose jet made it possible to move the center of gravity forward so that the longitudinal stability at a given lift coefficient could be greatly improved and flights could be made up to a lift coefficient of about 12.5. The lateral stability characteristics were generally satisfactory over the test range of lift coefficients except at angles of attack below about -5° where the Dutch roll oscillation became unstable. The model was flyable in the negative range of angles of attack, however, since the unstable lateral oscillation could be damped out by corrective lateral control. The longitudinal control provided by the all-movable horizontal tail and the lateral control provided by conventional ailerons and rudder were generally satisfactory at the lower lift coefficients; but, the control effectiveness decreased with increasing lift coefficient and was barely sufficient for maintaining flight at a lift coefficient of 12.5, even with large control deflections.

INTRODUCTION

Results of recent investigations made by the National Advisory Committee for Aeronautics (refs. 1 to 5) have indicated sufficient promise for jet-augmented-flap configurations to warrant a study of the dynamic stability and control characteristics at the very high lift coefficients that can be obtained with such flap arrangements. A flight-test investigation has, therefore, been made by the Langley Free-Flight-Tunnel Section with a sweptback-wing jet-transport airplane model equipped with an external-flow jet-augmented slotted flap.

The flight-test model used in the investigation was similar in geometry to the force-test model of references 4 and 5 and represented approximately a 1/20-scale model of a 200,000-pound jet-transport airplane with pod-mounted engines. Although the external-flow type of jet-augmented slotted flap was used on the model mainly for convenience, since such a flap arrangement has been found to be fairly easily applied to model configurations having pod-mounted engines, the results of the investigation are considered generally applicable for any type of jet-flap system.

The flight-test model of the present investigation was equipped with a partial-span jet-augmented-flap arrangement which was less efficient than the full-span flap used on the model of references 4 and 5. The flap of the model was also less efficient than some other external-flow jet-augmented-flap arrangements which have been tested. For example, an arrangement in which flat nozzles are used in combination with a specially designed double slotted flap has been found to be more efficient than the flap used in the present investigation. Since the main purpose of this investigation was to study the dynamic stability and control characteristics at very high lift coefficients, no attempt was made to increase the efficiency of this particular jet-augmented-flap arrangement. The flight tests covered a lift-coefficient range up to about 12 in order that the dynamic stability and control characteristics could be studied at the very high lift coefficients which could possibly be obtained with configurations of this type. It is highly unlikely, however, that lift coefficients as high as 12 can be achieved by subsonic jet-transport airplanes with flap arrangements of this type unless use is made of much higher thrust-weight ratios than are presently being considered for these airplanes. The maximum lift coefficients obtainable for subsonic jet-transport airplanes equipped with jet-augmented flaps are more likely to be in the range from 3 to 6.

The investigation consisted of flight tests made in the Langley full-scale tunnel at low speeds to determine the flight characteristics of the model in the flap-retracted and flap-extended configurations for

a range of lift coefficients from about 0.6 to about 12.5 and for a range of angles of attack from -12° to about 13° . A conventional horizontal-tail arrangement was used to provide longitudinal control over the test range of lift coefficients and also longitudinal trim except at very high lift coefficients where the tail became inadequate as a trim device. For tests at the very high lift coefficients, a downwardly directed nose jet was used to supplement the trimming power of the horizontal tail.

A limited number of force tests were made to determine the static stability and control characteristics of the flight-test model for the purpose of correlation with flight-test results.

SYMBOLS

The data are referred to the stability system of axes originating at a center of gravity located at 0.40 mean aerodynamic chord and on the fuselage reference line unless otherwise noted. (See fig. 1.)

b	wing span, ft
C_D	drag coefficient, Drag/qS
C_L	lift coefficient, Lift/qS
C_l	rolling-moment coefficient, M_{Xs}/qSb
$C_{l_\beta} = \frac{\partial C_l}{\partial \beta}$	per degree
$C_{l_{\delta a}}, C_{n_{\delta a}}, C_{Y_{\delta a}}$	aileron-effectiveness parameters
$C_{l_{\delta r}}, C_{n_{\delta r}}, C_{Y_{\delta r}}$	rudder-effectiveness parameters
C_m	pitching-moment coefficient, $M_{Ys}/qS\bar{c}$
C_n	yawing-moment coefficient, M_{Zs}/qSb
$C_{n_\beta} = \frac{\partial C_n}{\partial \beta}$	per degree

C_Y	lateral-force coefficient, F_{Ys}/qS
$C_{Y\beta} = \frac{\partial C_Y}{\partial \beta}$	per degree
C_μ	momentum coefficient based on thrust measured at nozzle, T/qS (For nose-jet arrangement, C_μ is based on total thrust at nozzle plus thrust of nose jet.)
c	chord, ft
\bar{c}	mean aerodynamic chord
F_D	drag force, lb
F_L	lift force, lb
F_{Ys}	lateral force, lb
i_t	angle of incidence of horizontal tail, deg
M_{Xs}	rolling moment, ft-lb
M_{Ys}	pitching moment, ft-lb
M_{Zs}	yawing moment, ft-lb
q	dynamic pressure, $\frac{1}{2}\rho V^2$, lb/sq ft
S	wing surface area, sq ft
T	thrust at nozzles, lb
V	velocity, ft/sec
X, Z	longitudinal and vertical body axes, respectively
X_s, Y_s, Z_s	longitudinal, lateral, and vertical stability axes, respectively
α	angle of attack of fuselage reference line, deg
β	angle of sideslip, deg

δ_a	aileron-deflection angle, deg
δ_e	elevator-deflection angle, deg
δ_f	geometric flap-deflection angle, measured in plane perpendicular to flap hinge line, deg
δ_r	rudder-deflection angle, deg
ϵ	angle between principal longitudinal axis of inertia and longitudinal body axis, positive when principal axis is below body axis at nose, deg
ρ	air density, slugs/cu ft
ψ	angle of yaw, deg

APPARATUS AND MODEL

Model

A drawing of the sweptback-wing jet-transport model used in the investigation is presented in figure 2, and a photograph of the model is shown in figure 3. Table I gives the dimensional and mass characteristics of the model. The wing of the model had 30° sweep of the quarter-chord, an aspect ratio of 6.56, and a taper ratio of 0.367. Pod-mounted engines were simulated by two nacelles attached to the wing on pylons. Each nacelle contained two air nozzles, and cold-air jets were used to simulate the jet-engine exhaust. The nose-jet arrangement used on the model (see fig. 2) consisted of a simple air nozzle directed downward at the nose. The nose jet and nacelles were supplied with compressed air from a common source through flexible hoses which passed internally through the model. The all-movable horizontal tail of the model was located about midspan of the vertical tail, had an area that was 25 percent of the wing area, and was equipped with a slotted flap to simulate an elevator.

The arrangement of the external-flow jet-augmented slotted flap used on the model was similar to that used in the tests of references 4 and 5 and is illustrated in figure 4. For take-off and landing, the jets from the pod-mounted engines are spread out into a horizontal sheet by retractable deflectors and are directed toward the base of the slotted flap which then turns the flattened jet sheet downward. The slotted flap was hinged on the bottom surface of the wing in such a

way that a smooth fairing was obtained between the upper surface of the slot and the lower surface of the wing for a flap deflection of 60° .

Flight-Test Equipment and Setup

The flight tests were made in the Langley full-scale tunnel. A sketch of the test setup is presented in figure 5, and a photograph of the model flying in the tunnel is shown in figure 6. In the flight-test setup there is an overhead safety cable to prevent the model from crashing. Combined with this cable is another cable composed of flexible plastic hoses which provide the compressed air for thrust and electrical conductors which provide power for the control actuators. These cables are attached to the model at about the center-of-gravity location. The control actuators are energized remotely by means of control sticks which are used by the pilots to apply corrective control to the model. Flicker-type (full-on or full-off) control is used in flying the model, and trim of the control surfaces is provided by small electric motors or trimming devices built into the actuators. The pitch pilot, located by the side of the test section, controls the longitudinal motions of the model by deflecting the horizontal tail or elevator for control or trim. The thrust controller, also located by the side of the test section, varies the thrust of the model by remotely controlling the air flow to the model through a valve located at the top of the entrance cone. The safety-cable operator adjusts the safety cable so that it can be slack during flight and takes up the slack to prevent the model from crashing if it goes out of control. A second pilot who controls the rolling and yawing motions of the model is located near the bottom of the exit cone. Motion-picture records of the flights are obtained with cameras located at the side of the test section and at the top and bottom of the exit cone.

The flight-test technique employed with this setup can best be explained by describing a typical flight. A flight is started with the model being towed by the safety cable. When the tunnel air velocity reaches the desired flying speed for the model, thrust is increased until the flight cable becomes slack. Adjustments to the horizontal-tail incidence and thrust are then made, if necessary, to trim the model for the particular airspeed. The flight is then continued to higher or lower airspeeds by remotely changing the angle of incidence of the horizontal tail and by making the necessary adjustments to tunnel speed and model thrust to maintain steady flight.

DETERMINATION OF STATIC STABILITY AND CONTROL

CHARACTERISTICS OF FLIGHT-TEST MODEL

Reduction of Force-Test Data

The force tests of the investigation were made in the Langley full-scale tunnel. All force tests were made with a vertical-strut support system and strain-gage balances. The test setup was located in the forward portion of the test section near the lower lip of the entrance cone. No wind-tunnel corrections have been applied to the data since the model was relatively small compared with the size of the tunnel test section.

The momentum coefficient C_μ used in this report is defined as T/qS . For the basic model, T is the thrust at the nozzles as determined from force tests. For the nose-jet arrangement, T is the total thrust of the nozzle plus the thrust of the nose jet. This coefficient is approximately equivalent to the momentum coefficient C_μ which has been used in boundary-layer-control investigations and in the jet-augmented-flap investigations reported in references 1, 2, and 3. In order to determine thrust losses in spreading and deflecting the jet, values of thrust were obtained from force measurements made during static calibrations of the cruising condition (flaps and deflectors retracted) and of the landing condition (flaps and deflectors extended). Comparison of the calibration data for these two conditions indicated that the losses caused by spreading and deflecting the jet were about 25 percent for the flap deflection of 60° and about 30 percent for the flap deflection of 70° .

Static Longitudinal Stability and Trim Characteristics

Force tests were made to determine the static longitudinal stability and trim characteristics of the model in the flap-retracted and flap-extended conditions for a range of angles of attack from -8° to 12° . Flap-deflection angles of 0° , 50° , and 70° were investigated for a range of momentum coefficients up to about 11.20. Trim studies were made for angles of incidence of the horizontal tail of 10° and 20° and also for an arrangement in which a downwardly directed nose jet was used to supplement the trimming power of the horizontal tail. All the force tests were conducted for a range of dynamic pressures from about 0.26 to about 1.6 pounds per square foot which corresponds to a velocity range from about 15 to about 37 feet per second and to a Reynolds number range from about 103,000 to about 250,000, based on the mean aerodynamic chord of the wing.

Flaps and deflectors retracted.- The static longitudinal stability and trim characteristics of the model in the cruising condition (flaps and deflectors retracted) are presented in figure 7. These data, which were obtained with power off, indicate a fairly linear variation of pitching moment with lift coefficient for the test range of angles of attack and show that the model had about 20-percent static margin with the center of gravity located at 0.40 mean aerodynamic chord.

Flaps and deflectors extended.- The data for the model in the landing condition (flaps and deflectors extended) are presented in figures 8 to 10. The data for the configuration with horizontal tail off (fig. 8) are presented for a flap deflection of 50° and show variations in pitching-moment characteristics similar to those shown in references 4 and 5. The pitch-up at positive angles of attack is not associated directly with the jet-augmented flap but is characteristic of swept wings of high aspect ratio with inboard partial-span flaps.

The data for the configuration with horizontal tail on are presented in figures 9 and 10. The data of figure 9 are presented for a flap deflection of 50° , for an elevator deflection of -20° , and for angles of incidence of the horizontal tail of 10° and 20° . These data, which are applicable to the flight-test conditions in which only the horizontal tail is used for longitudinal trim, show that the horizontal tail provided both trim and stability at the lower lift coefficients. Although the stability of the model decreased with increasing lift coefficient, the horizontal tail appeared to provide trim and at least marginal stability up to a lift coefficient of about 4 for both the negative and small positive range of angles of attack. Trim and stability above this lift coefficient were not possible with this particular horizontal-tail arrangement. The drag data of figure 9 indicate that flap deflections higher than 50° are necessary for steady level flight near zero angle of attack for lift coefficients of 4 and above.

Presented in figure 10 are the results of tests made to simulate the flight conditions in the very high lift-coefficient range in which a nose jet was used to supplement the trimming power of the horizontal tail. These data are presented for a flap deflection of 70° , for an elevator deflection of 0° , and for an angle of incidence of the horizontal tail of 20° . The pitching-moment data, which are referred to 0.30 mean aerodynamic chord, indicate about neutral static longitudinal stability for lift coefficients of about 12 or 13. For the conditions shown, the nose jet provided more than enough positive increment of pitching moment for trim at these high lift coefficients with little or no effect on the longitudinal stability characteristics.

Static Lateral Stability Characteristics

A few force tests were made to determine the static lateral stability characteristics of the model for the conditions covered in the flight-test investigation. The results of these tests are presented in figure 11 in the form of the static-lateral-stability parameters $C_{Y\beta}$, $C_{n\beta}$, and $C_{l\beta}$ plotted against lift coefficient for flap deflections of 50° and 70° . Data points have also been plotted in this figure for the flap-retracted, cruising condition and for the 70° flap-extended configuration in which a nose jet was used to provide trim. All these data were measured at an angle of attack of 0° , at an angle of incidence of the horizontal tail of 20° , and at angles of sideslip of $\pm 10^\circ$. The variation of C_Y , C_n , and C_l with angle of sideslip was fairly linear up to angles of sideslip of $\pm 10^\circ$.

The data of figure 11 show that in the range of low lift coefficients the flap-extended configuration had about the same values of positive directional stability $C_{n\beta}$ and positive effective dihedral $-C_{l\beta}$ as those of the flap-retracted configuration ($C_{n\beta} = 0.0025$; $C_{l\beta} = -0.0025$). As the lift coefficient was increased (by increasing C_μ), both the 50° and 70° flap-extended configurations showed an increase in $C_{n\beta}$ and $-C_{l\beta}$. At the highest test lift coefficient, the 70° flap-extended configuration had values of $C_{n\beta}$ of about 0.0055 and of $C_{l\beta}$ of about -0.0085 which were approximately two or three times as large as those at low lift coefficients. The data points plotted in figure 11 to represent the nose-jet configuration show little or no effect of the nose jet on the static-lateral-stability parameters.

Static Lateral Control Characteristics

Tests were made to determine the aileron effectiveness (fig. 12(a)) and rudder effectiveness (fig. 12(b)) for the test range of lift coefficients for flap deflections of 50° and 70° at an angle of attack of 0° , angle of sideslip of 0° , and angle of incidence of the horizontal tail of 20° . Data points for the flap-retracted configuration are also plotted in this figure for purposes of comparison. These data were measured for control deflections which were generally representative of those used in the flight tests. For the flap-retracted configuration these control deflections were $\pm 7.5^\circ$ for the ailerons and $\pm 10^\circ$ for the rudder. For

the flap-extended configuration, these control deflections varied from $\pm 15^\circ$ for the ailerons and $\pm 10^\circ$ for the rudder for a flap deflection of 50° to $\pm 20^\circ$ for the ailerons and rudder for a flap deflection of 70° .

The data of figure 12(a) show that at low lift coefficients the aileron-effectiveness parameter $C_{l_{\delta a}}$ for the flap-extended configuration ($C_{l_{\delta a}}$ from about 0.0006 to 0.0008) was somewhat lower than that for the flap-retracted configuration ($C_{l_{\delta a}}$ of about 0.001). The value of $C_{l_{\delta a}}$ for the flap-extended configuration generally increased with increasing lift coefficient. At the highest lift coefficients in the investigation, a flap deflection of 70° produced values of $C_{l_{\delta a}}$ which were considerably larger than those in the range of low lift coefficients. The yawing moment produced by aileron deflection was generally favorable for the lift-coefficient range in the investigation.

The data of figure 12(b) show that at low lift coefficients the rudder-effectiveness parameter $C_{n_{\delta r}}$ for the 50° flap-extended configuration was about the same as that for the flap-retracted configuration. An increase in lift coefficient produced an initial rapid increase in the values of $C_{n_{\delta r}}$ for this configuration but showed no consistent effect on $C_{n_{\delta r}}$ in the higher lift-coefficient range. The values of $C_{n_{\delta r}}$ for the 70° flap-extended configuration were considerably lower than those for the 50° flap-extended configuration and remained about constant up to the highest test lift coefficient.

FLIGHT TESTS

Flight tests were made to determine the stability and control characteristics and general flight behavior of the model over a lift-coefficient range from 0.6 to 0.9 for the flap-retracted configuration and over a lift-coefficient range up to 12.5 for the flap-extended configuration. Most of the flights were made in the low positive range of angles of attack, but one series of flights was made for a range of angles of attack from -12° to 13° to determine the effect of angle of attack on the flight characteristics of the model at a lift coefficient of 7.5.

The model was flown up to a lift coefficient of 6 without the nose jet. Most of the flights without the nose jet were made with the center of gravity located at 0.40 mean aerodynamic chord to reduce the positive pitching moment that the horizontal tail had to provide for trim. A few flights without the nose jet were made with the center of gravity located at 0.35 mean aerodynamic chord. For flights with the nose jet operating, the center of gravity was moved forward to 0.30 mean aerodynamic chord for increased static longitudinal stability. Flights at this forward center-of-gravity location were possible up to a lift coefficient of 12.5 because use of the nose jet made it possible to provide enough positive pitching moment to trim out the large diving moment of the jet-augmented flap. The nose jet and nacelles were supplied with compressed air from a common source so that an increase or decrease in the diving moment of the jet-augmented flap as a result of thrust changes could be accompanied by an opposite variation in the nose-up pitching moment provided by the nose jet. The nose jet was used for trim only, however, and longitudinal control was obtained by deflection of the all-movable horizontal tail.

The model was flown with coordinated rudder and aileron flicker-type (full-on or full-off) control. The control deflections used for the cruising condition were $\pm 9^\circ$ for the rudder, $\pm 7.5^\circ$ for the ailerons, and $\pm 5^\circ$ for the horizontal tail. The control deflections were generally increased as the tunnel speed was reduced; at a lift coefficient of 12.5 the control deflections were $\pm 20^\circ$ for the rudder, $\pm 20^\circ$ for the ailerons, and $\pm 20^\circ$ for the horizontal tail.

The model behavior during flight was observed by the pitch pilot located at the side of the test section and by the roll-and-yaw pilot located in the rear of the test section. The flight-test data were obtained from the pilots' observations and motion-picture records made during the flights, and the flight-test results presented in the following section are based on these observations and motion-picture records.

FLIGHT-TEST RESULTS AND DISCUSSION

A motion-picture film supplement covering the flight tests of the model has been prepared and is available on loan. A request-card form and a description of the film will be found at the back of this report, on the page immediately preceding the abstract and index page.

Longitudinal Stability Characteristics

Flaps and deflectors retracted.- In the cruising condition (flaps and deflectors retracted) the model was found to have satisfactory longitudinal stability and control characteristics over the lift-coefficient range in the investigation (0.6 to 0.9) with the center of gravity located at 0.40 mean aerodynamic chord. The model was also flown in the flap-retracted configuration with the deflectors extended; in this configuration, the jets from the pod-mounted engines were deflected up to the bottom of the wing and spread out in the form of a flat sheet. Flight characteristics of the model in this configuration were generally similar to those of the model with the deflectors retracted.

Flaps extended (without nose jet).- The range of lift coefficients, angles of attack, and flap deflections covered in the flight tests of the flap-extended configuration without the nose jet are presented in figure 13(a). This configuration was flown over a range of lift coefficients up to 6, of angles of attack from 1.5° to 10° , and of flap deflections up to 50° . The longitudinal stability characteristics were found to be satisfactory for the test conditions up to a lift coefficient of about 4, and extending the flaps to 15° and 30° produced no apparent adverse effect on the longitudinal stability characteristics for the test range of angles of attack. Satisfactory flights were also made for the 50° flap-extended configuration at an angle of attack of 1.5° , but at angles of attack of 4° and 8° the model exhibited a nose-up tendency because of static longitudinal instability. As already pointed out in the discussion of force-test data, this instability is not associated directly with the jet-augmented flap. Although the jet-augmented flap reduced the longitudinal stability, the longitudinal pitch-up is characteristic of sweptback wings of high aspect ratio with inboard partial-span flaps. Sustained flights to lift coefficients higher than about 4 at low angles of attack (which required flap deflections larger than 50°) could not be made because more trimming power was required of the horizontal tail than the tail could produce. Flights of limited duration could be made at lift coefficients of 5 and 6, however, by flying the model at moderate angles of attack where the pitch-up tendency effectively reduced the amount of nose-up trim required of the horizontal tail. The longitudinal instability of these conditions required constant attention to the elevator control to maintain flight.

Flaps extended (with nose jet).- The flap-extended configuration with the nose jet was flown over a range of lift coefficients up to 12.5, of angles of attack from -12° to 13° , and of flap deflections up to 75° . (See fig. 13(b).) For these flight tests, the center of gravity was moved forward from 0.40 to 0.30 mean aerodynamic chord to obtain

increased static longitudinal stability. The longitudinal stability characteristics of this configuration were found to be generally better than those without the nose jet, apparently because of the increase in static margin.

Unlike the flap-extended configuration without the nose jet, the model with the nose-jet arrangement could be trimmed to fly at lift coefficients higher than about 4 at low angles of attack where the pitch-up tendency did not occur. By increasing the flap angle from 50° up to 70° and by trimming out the large diving moments with the nose jet, flights were made up to a lift coefficient of about 12.5 at angles of attack near 0° . The flight characteristics of this configuration were found to be generally satisfactory at moderate lift coefficients, but the longitudinal stability appeared to decrease with increasing lift coefficient and to become marginal at the highest lift coefficient of the investigation where constant attention was required on the elevator control to maintain flight.

The data of figure 13(b) show the flight-test points which were covered to study the effect of angle of attack on the longitudinal stability characteristics of the model. These tests were made at a lift coefficient of 7.5 and for a range of angles of attack from -10° (flap deflection of 75°) to 13° (flap deflection of 50°). The longitudinal stability characteristics of the model at this lift coefficient were found to be generally satisfactory over the range of negative and small positive angles of attack. At an angle of attack of 8° the model exhibited a pitch-up tendency which was difficult to control. At an angle of attack of 13° the pitch-up was so violent that only short-distance flights could be made.

Longitudinal Control Characteristics

The longitudinal control characteristics of the model without the nose jet were generally satisfactory at the lower lift coefficients. As the lift coefficient increased, the horizontal-tail load required for trim progressively increased until, at lift coefficients between about 4 and 6, the maximum tail load was realized and no positive pitching moment was available for control. As a result, the elevator pilot had no control for stopping a diving motion of the model.

The longitudinal control characteristics of the model with the nose jet were generally satisfactory at the lower lift coefficients; but, the control effectiveness appeared to decrease with increasing lift coefficient and, at lift coefficients near 12.5, was barely sufficient for maintaining flight, even when large control deflections were used.

Lateral Stability Characteristics

The lateral stability characteristics of the model in the clean condition were found to be satisfactory, and no adverse effect was apparent on the lateral stability characteristics when the deflectors were extended so that the jet exhaust could be deflected up to the bottom of the wing and spread out in the form of a flat jet sheet.

The lateral stability characteristics of the flap-extended configuration without the nose jet were satisfactory for angles of attack from 1.5° to 10° (lift coefficients up to about 6). No attempt was made to fly this configuration at negative angles of attack.

The lateral stability characteristics of the flap-extended configuration with the nose jet were found to be satisfactory at small negative angles of attack and over the positive test range of angles of attack for lift coefficients up to 12.5. Flights made at a lift coefficient of 7.5 to study the effect of angle of attack on the flight characteristics of the model indicated that below an angle of attack of about -5° the Dutch roll oscillation became unstable because of the unfavorable inclination of the longitudinal principal axis of inertia. The model was flyable in the negative range of angles of attack, however, even down to angles of attack of -10° ($C_L = 7.5$) and -12° , since the unstable lateral oscillation could be damped out by corrective lateral control.

Lateral Control Characteristics

The lateral control characteristics of the model were generally satisfactory at the lower lift coefficients investigated but both the aileron- and rudder-control effectiveness appeared to decrease with increasing lift coefficient. At a lift coefficient of 12.5, the lateral-control effectiveness was barely adequate for controlling the model, even with large control deflections and with the relatively large values of $C_{l_{\delta a}}$ indicated by the force-test data of figure 12(a).

The increase in rolling-moment coefficient with increasing lift coefficient was more than offset by the reduction in dynamic pressure over the ailerons, and the rolling moment produced by the ailerons was actually smaller at the high lift coefficients.

Although most flights of the model were made with a neutral aileron position of 0° , a few flights were made at lift coefficients up to about 4 with the ailerons deflected down to 25° . For this condition, increased rudder deflection was required to counteract the adverse yawing moment of the ailerons.

One difficulty which was encountered in flying the model at high lift coefficients was that of large out-of-trim yawing and rolling moments which resulted from model asymmetry or asymmetrical thrust conditions. It was necessary in the flight tests to eliminate these out-of-trim moments by making proper adjustments to the model thrust and flap settings so that flights could be made at an angle of sideslip of 0° over the lift-coefficient range of the investigation.

A study of asymmetrical thrust conditions that might result from engine failure was beyond the scope of this investigation. It is apparent, of course, that engine failure can introduce serious out-of-trim yawing and rolling moments for an airplane of the type investigated. The severity of the problem depends on many factors such as the number and location of the engines installed in the airplane, the type of control system used, and the increment of lift provided by jet augmentation.

SUMMARY OF RESULTS

From a wind-tunnel investigation made at low speeds to determine the flight characteristics of a model of a sweptback-wing jet-transport airplane equipped with an external-flow jet-augmented slotted flap and with a downwardly directed nose jet to supplement the trimming power of the horizontal tail at very high lift coefficients, the following results may be summarized:

1. The model was flown up to a lift coefficient of 6 without the nose jet, but the longitudinal stability was considered satisfactory only at lift coefficients below about 4. The use of the nose jet made it possible to move the center of gravity forward so that the longitudinal stability at a given lift coefficient could be greatly improved and flights could be made up to a lift coefficient of about 12.5.
2. The lateral stability characteristics were generally satisfactory over the test range of lift coefficients except at angles of attack below about -5° where the Dutch roll oscillation became unstable. The model was flyable in the negative range of angles of attack, however, since the unstable lateral oscillation could be damped out by corrective lateral control.
3. The longitudinal control provided by the all-movable horizontal tail and the lateral control provided by conventional ailerons and rudder were generally satisfactory at the lower lift coefficients; but, the control effectiveness decreased with increasing lift coefficient

and was barely sufficient for maintaining flight at a lift coefficient of 12.5, even with large control deflections.

Langley Aeronautical Laboratory,
National Advisory Committee for Aeronautics,
Langley Field, Va., March 11, 1958.

REFERENCES

1. Lockwood, Vernard E., Turner, Thomas R., and Riebe, John M.: Wind-Tunnel Investigation of Jet-Augmented Flaps on a Rectangular Wing to High Momentum Coefficients. NACA TN 3865, 1956.
2. Lowry, John G., and Vogler, Raymond D.: Wind-Tunnel Investigation at Low Speeds To Determine the Effect of Aspect Ratio and End Plates on a Rectangular Wing With Jet Flaps Deflected 85° . NACA TN 3863, 1956.
3. Vogler, Raymond D., and Turner, Thomas R.: Wind-Tunnel Investigation at Low Speeds To Determine Flow-Field Characteristics and Ground Influence on a Model With Jet-Augmented Flaps. NACA TN 4116, 1957.
4. Campbell, John P., and Johnson, Joseph L., Jr.: Wind-Tunnel Investigation of an External-Flow Jet-Augmented Slotted Flap Suitable for Application to Airplanes With Pod-Mounted Jet Engines. NACA TN 3898, 1956.
5. Johnson, Joseph L., Jr.: Wind-Tunnel Investigation of the Static Longitudinal Stability and Trim Characteristics of a Sweptback-Wing Jet-Transport Model Equipped With an External-Flow Jet-Augmented Flap. NACA TN 4177, 1958.

TABLE I.- DIMENSIONAL AND MASS CHARACTERISTICS OF MODEL

Weight, lb	21.4
Wing loading, Weight/S, lb/sq ft	3.09
Moment of inertia about X-axis, slug-ft ²	0.51
Moment of inertia about Z-axis, slug-ft ²	2.25
ϵ , deg	6
Wing:	
Area, sq ft	6.95
Aspect ratio	6.56
Mean aerodynamic chord, ft	1.10
NACA airfoil section, root	65 ₁ -412
NACA airfoil section, tip	65 ₁ -412
Flap chord, percent wing chord	25.0
Flap span, percent wing span	67.0
Root chord, ft	1.5
Tip chord, ft	0.55
Span, ft	6.75
Taper ratio	0.367
Sweep of quarter-chord, deg	30
Incidence, deg	0
Twist, deg	0
Horizontal tail:	
Area (total), sq ft	1.74
Length (distance from 0.40 \bar{c} of wing to 0.25 \bar{c} of tail), ft	2.93
Span, ft	2.87
Root chord, ft	0.96
Tip chord, ft	0.31
Mean aerodynamic chord, ft	0.69
Aspect ratio	4.73
Sweep of leading edge, deg	38
Taper ratio	0.323
NACA airfoil section	65-009
Vertical tail:	
Exposed area, sq ft	1.31
Exposed span, ft	1.45
Root chord at fuselage intersection, ft	1.17
Tip chord, ft	0.63
Sweep of leading edge, deg	30
NACA airfoil section	65-009

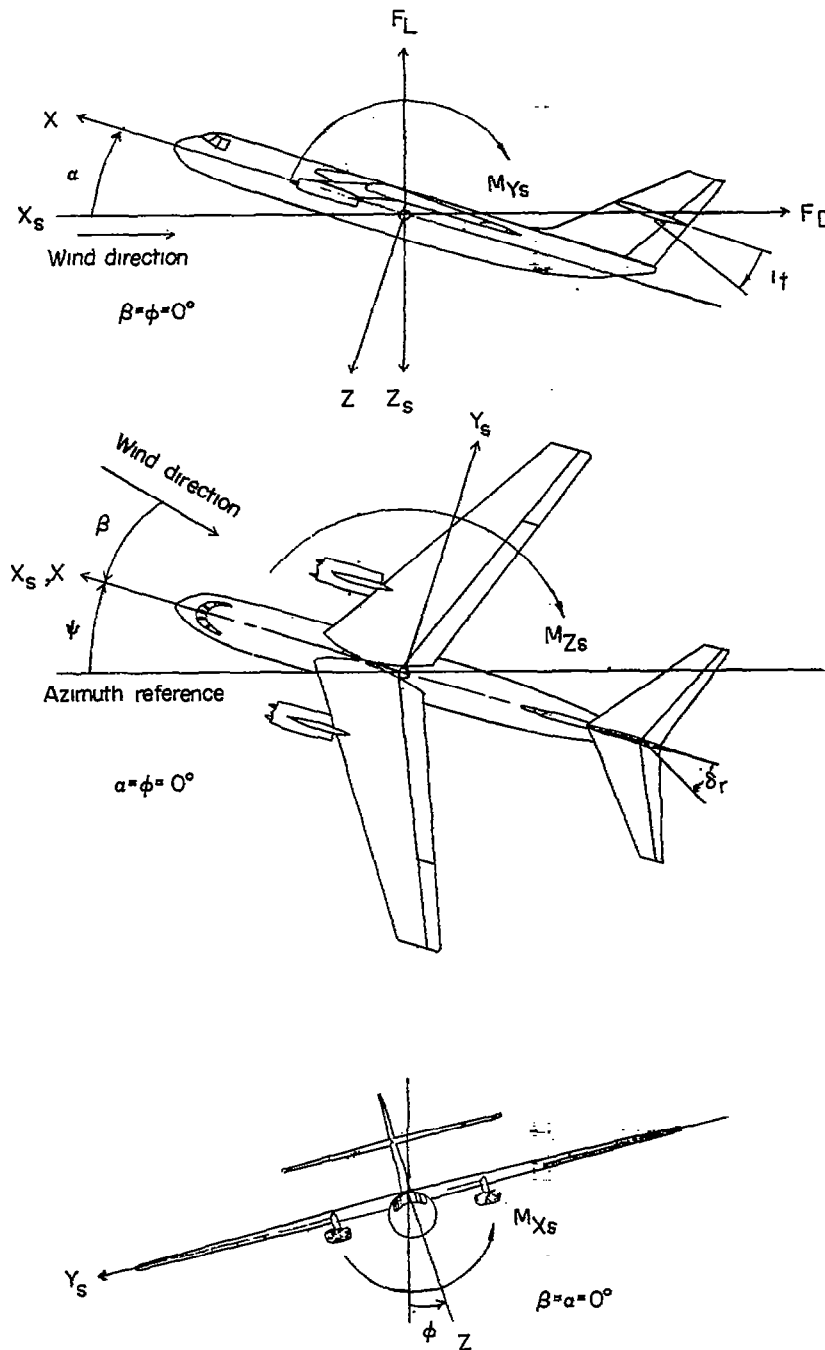


Figure 1.- System of axes used in the investigation. All force-test data are referred to the stability system of axes. Arrows indicate positive directions of moments, forces, and angles.

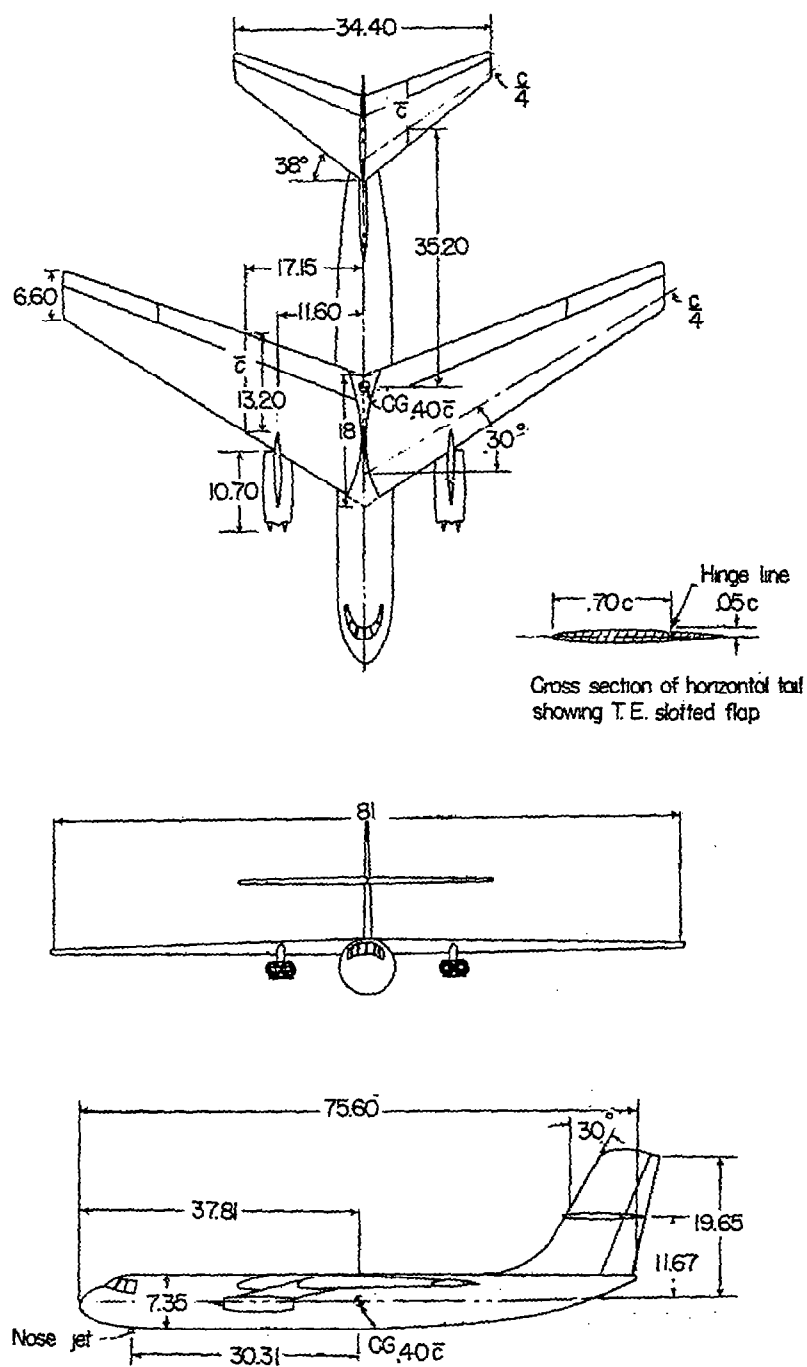


Figure 2.- Three-view drawing of sweptback-wing jet-transport airplane model used in investigation. All dimensions are in inches unless otherwise specified.

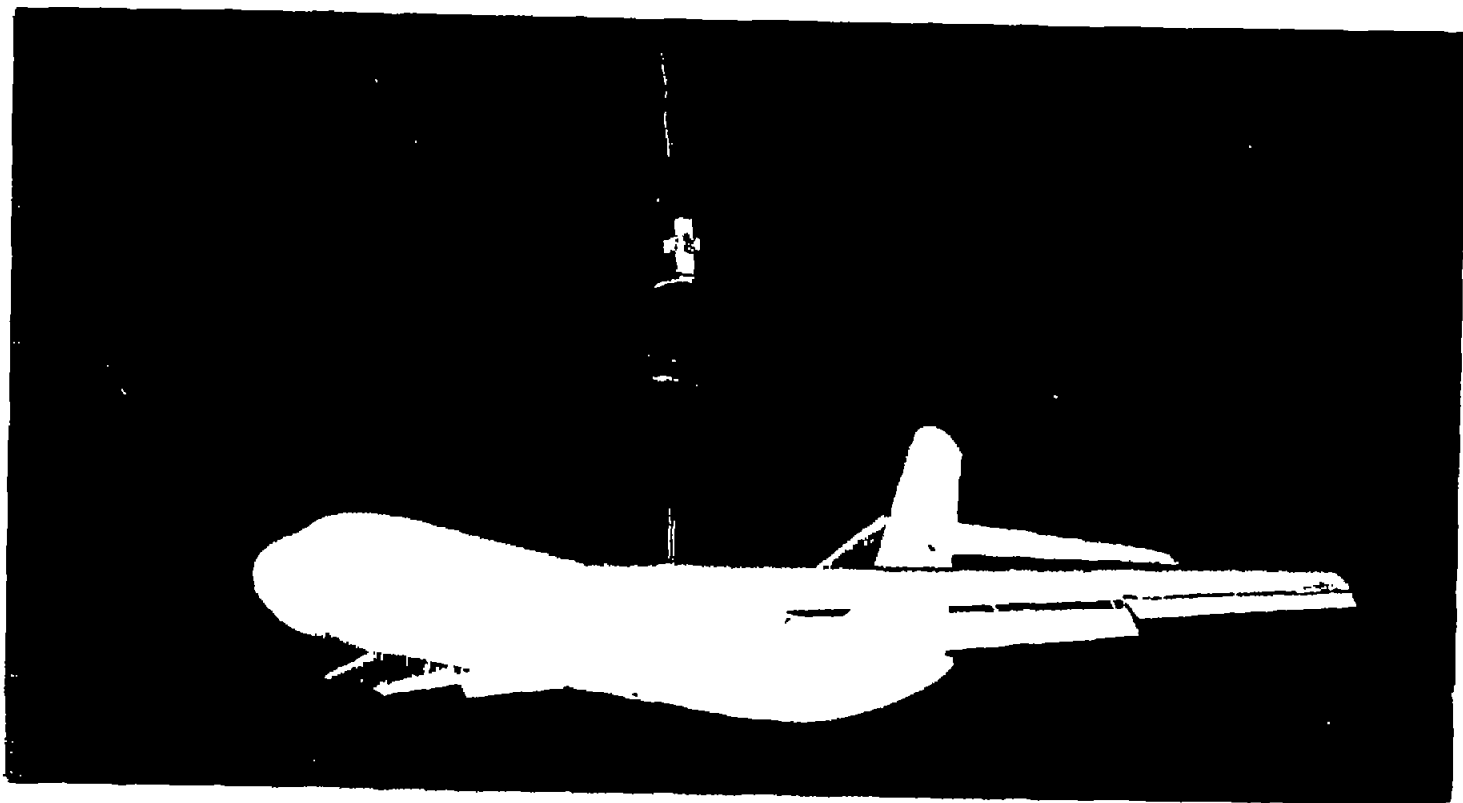
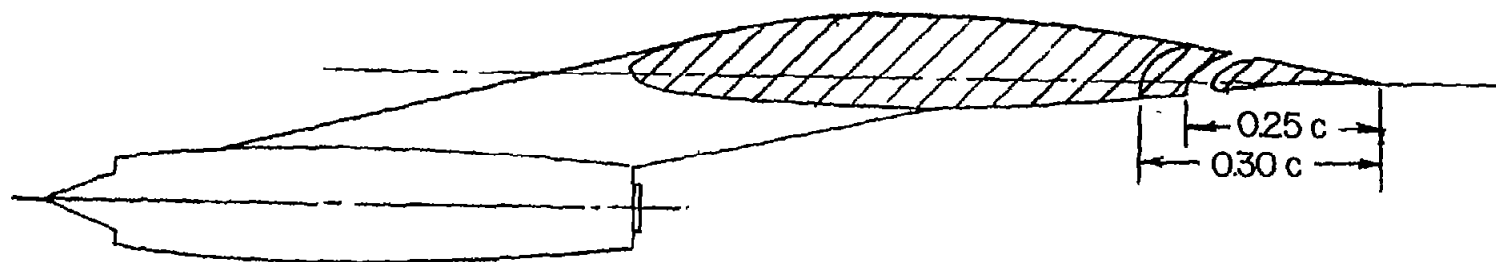
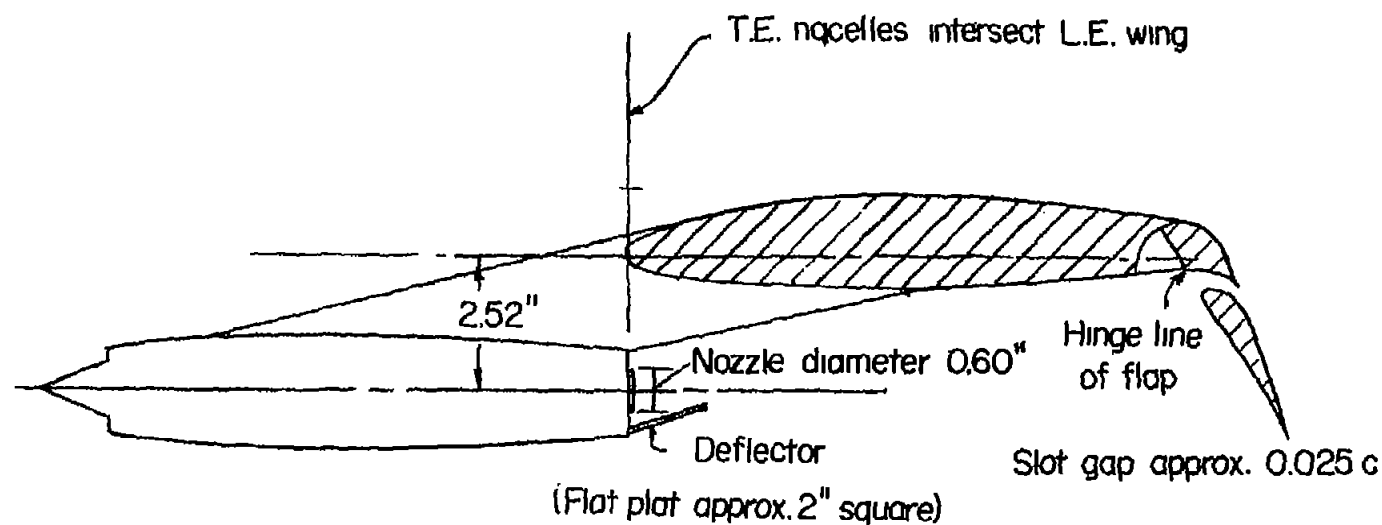


Figure 3.- Photograph of model used in investigation. L-96535



(a) Cross section of wing in cruising condition.



(b) Cross section of wing in landing condition.

Figure 4.- Arrangement of external-flow jet-augmented slotted flap used in investigation.

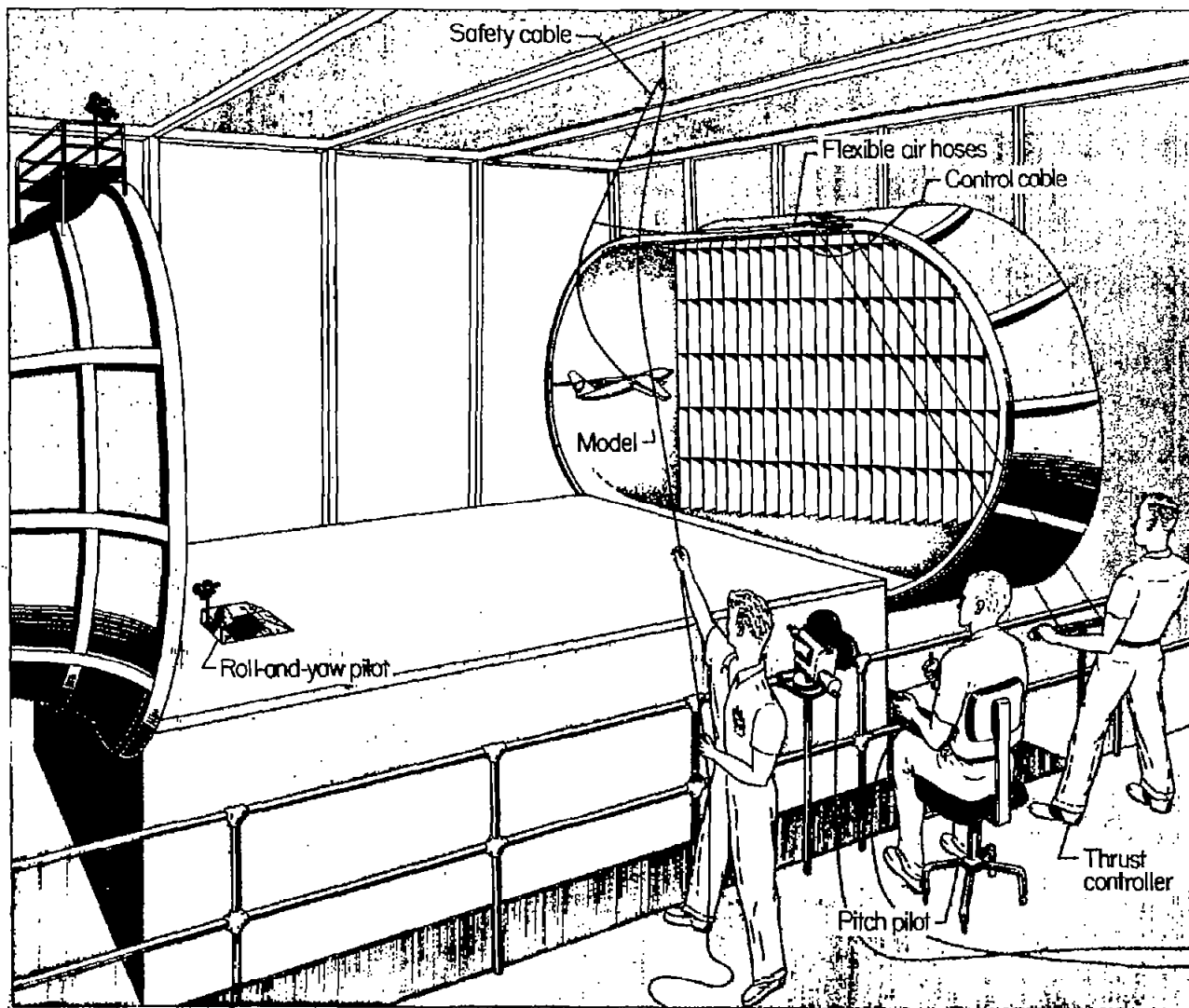


Figure 5.- Sketch of flight-test setup in the Langley full-scale tunnel.

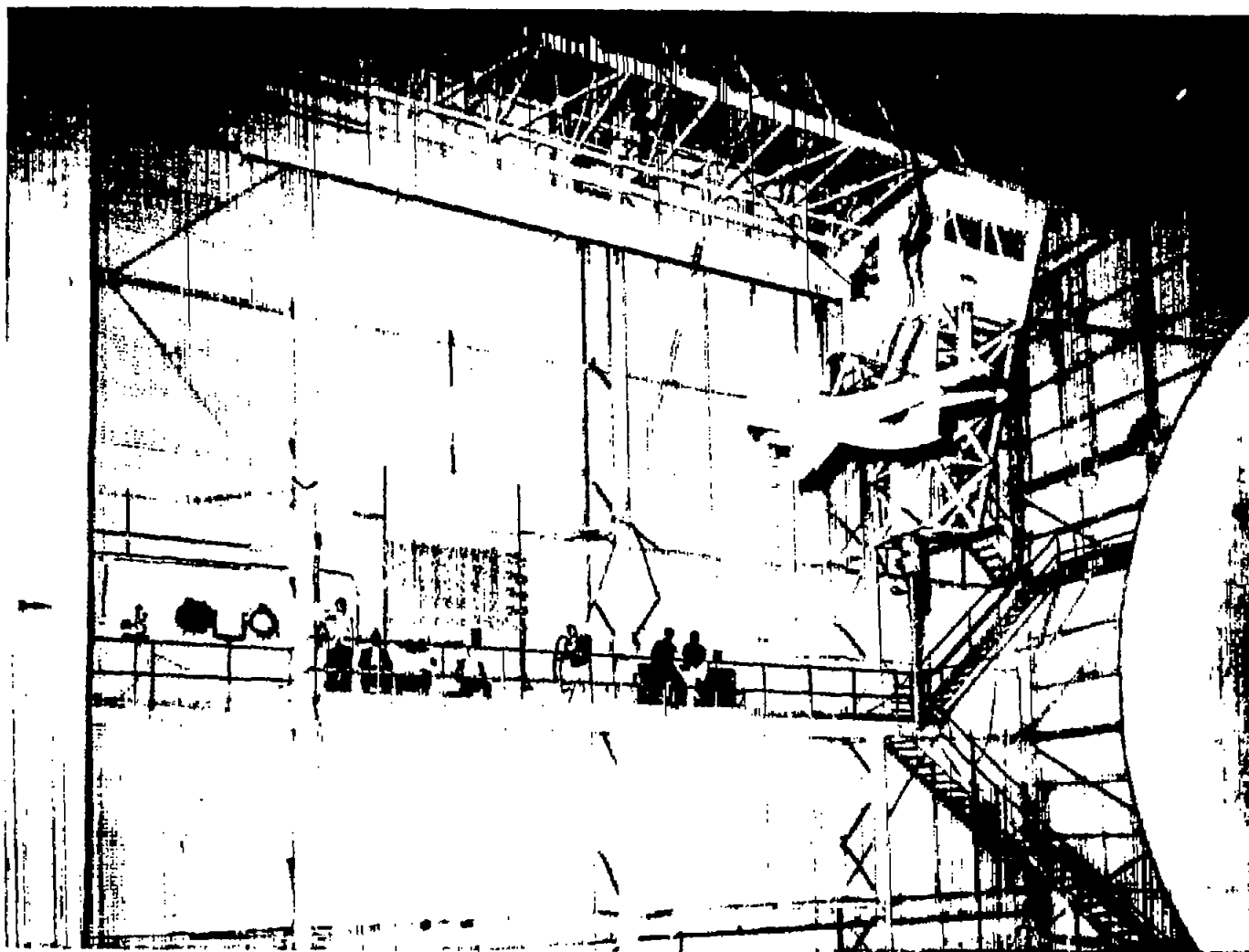


Figure 6.- Photograph of model flying in test section of the Langley full-scale tunnel.

L-96826

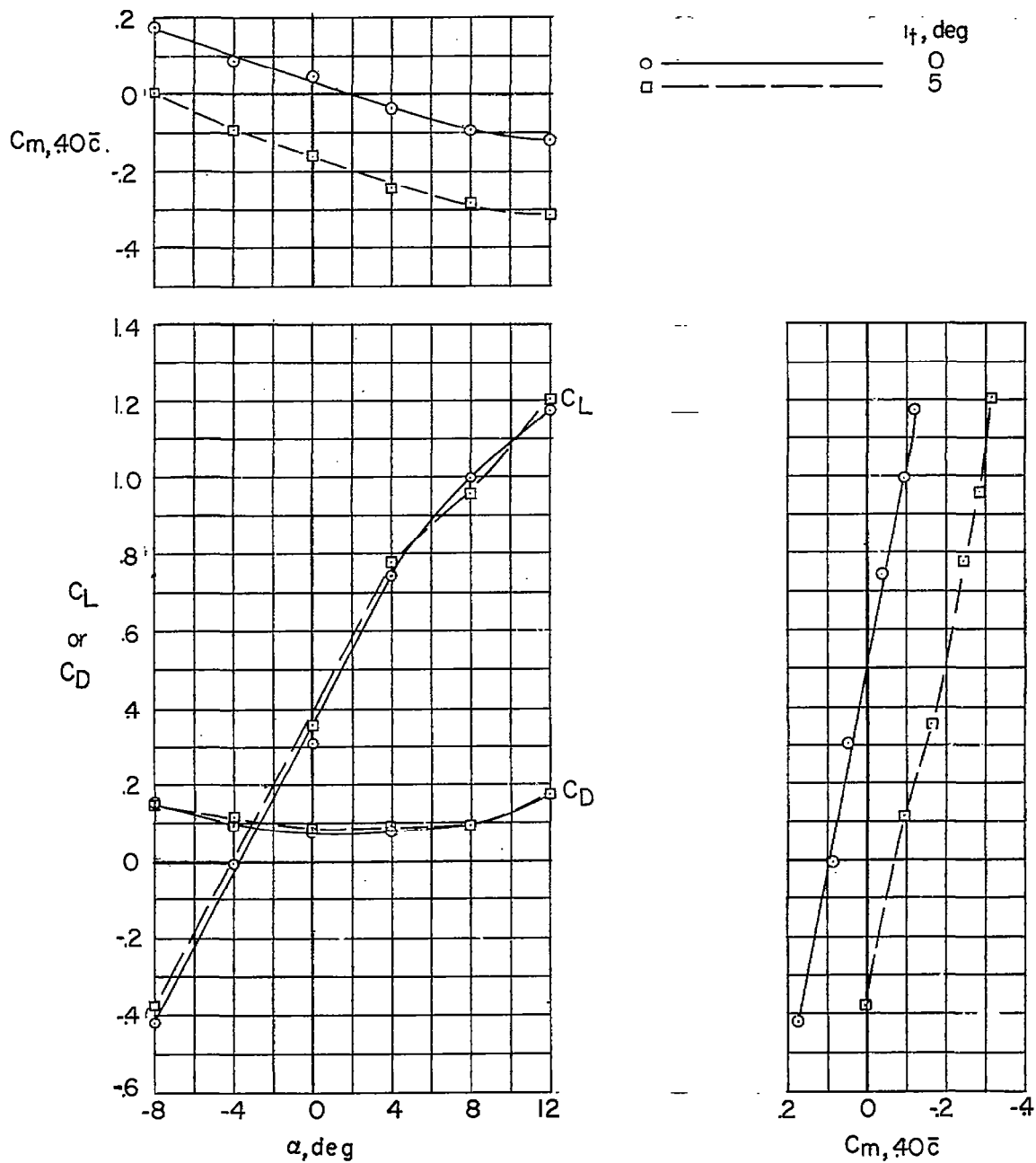


Figure 7.- Static longitudinal stability and trim characteristics of the model in the cruising condition. Flaps and deflectors retracted; $\delta_e = 0^\circ$.

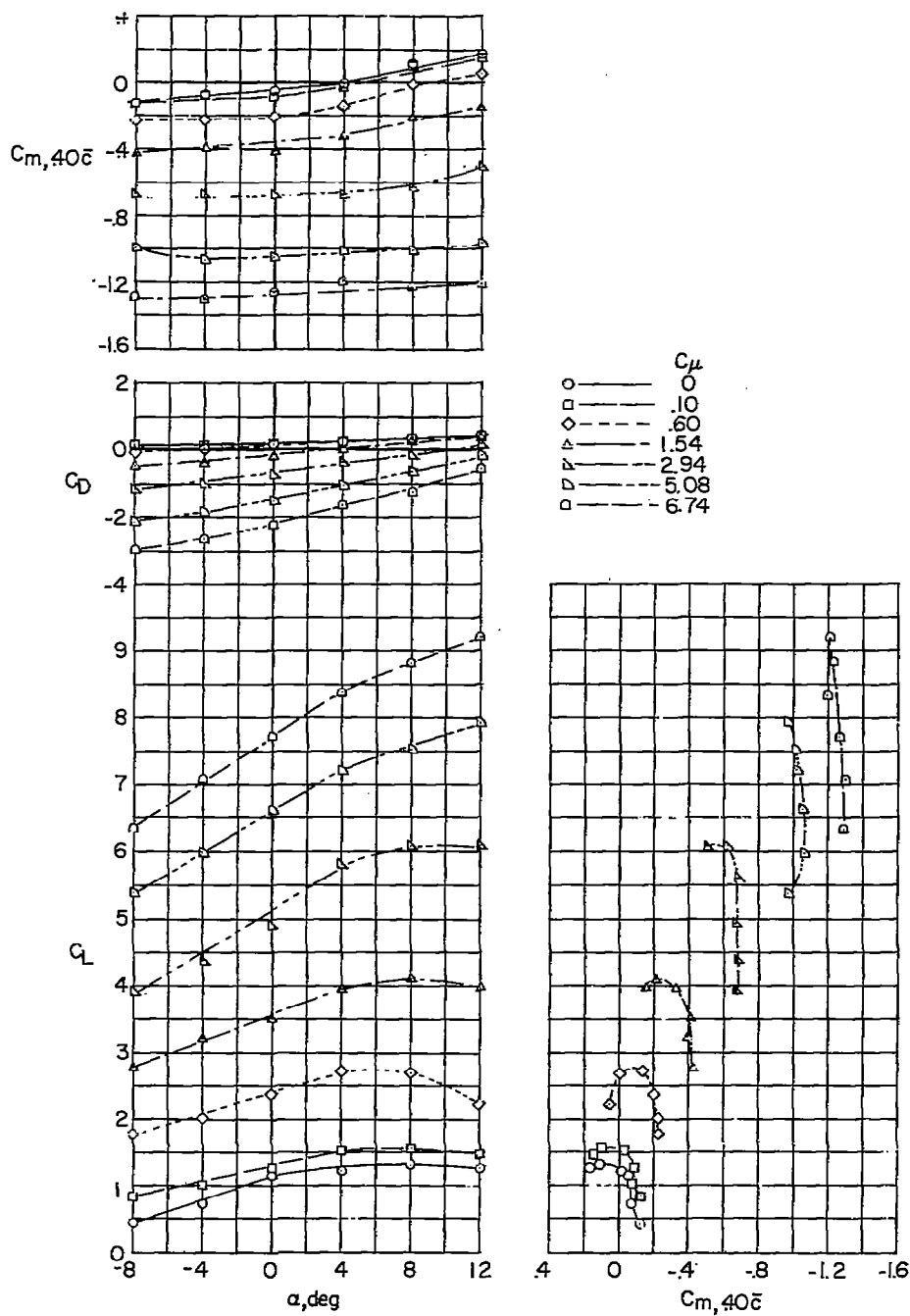
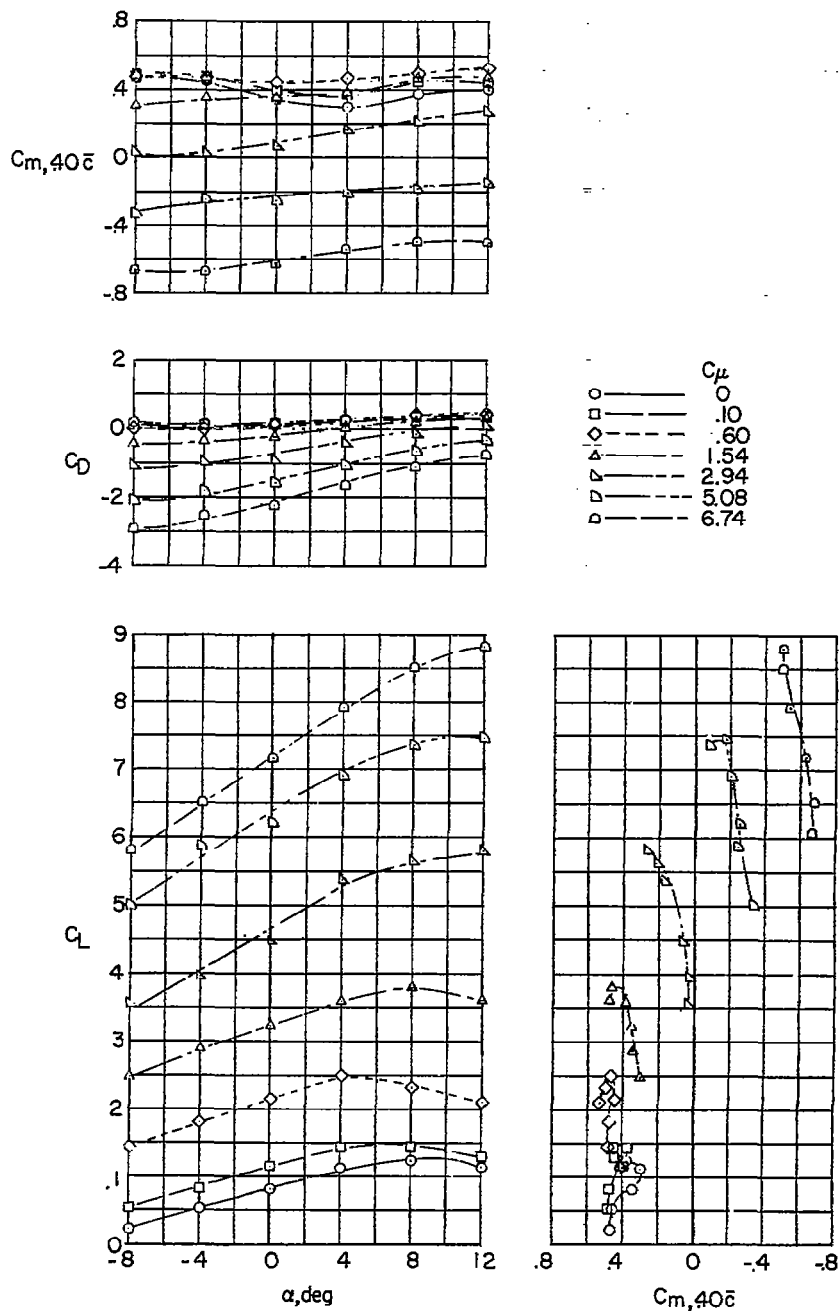
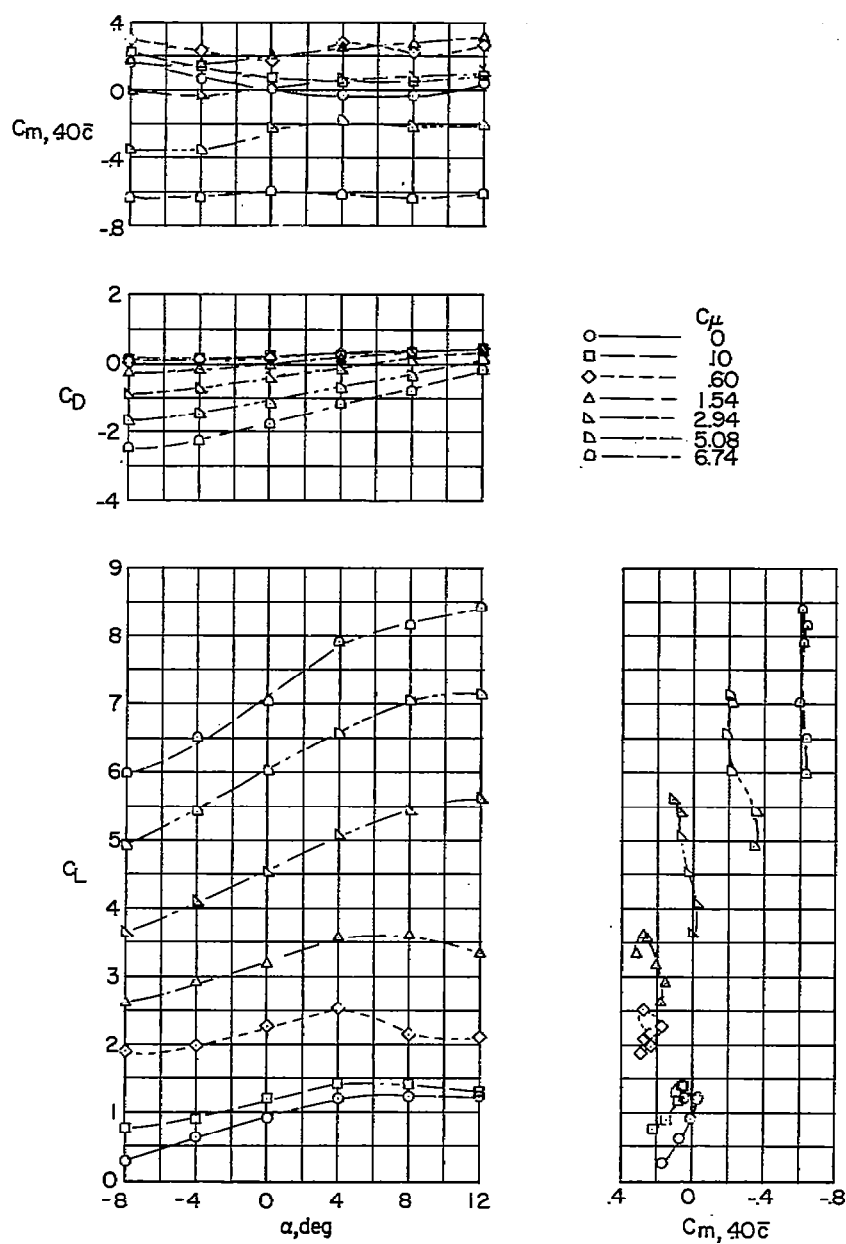


Figure 8.- Static longitudinal stability and trim characteristics of the model in the landing condition. Flaps and deflectors extended; $\delta_f = 50^\circ$; horizontal tail off.



(a) $i_t = 10^\circ$.

Figure 9.- Static longitudinal stability and trim characteristics of the model in the landing condition. $\delta_f = 50^\circ$; $\delta_e = -20^\circ$; horizontal tail on.



(b) $i_t = 20^\circ$.

Figure 9.- Concluded.

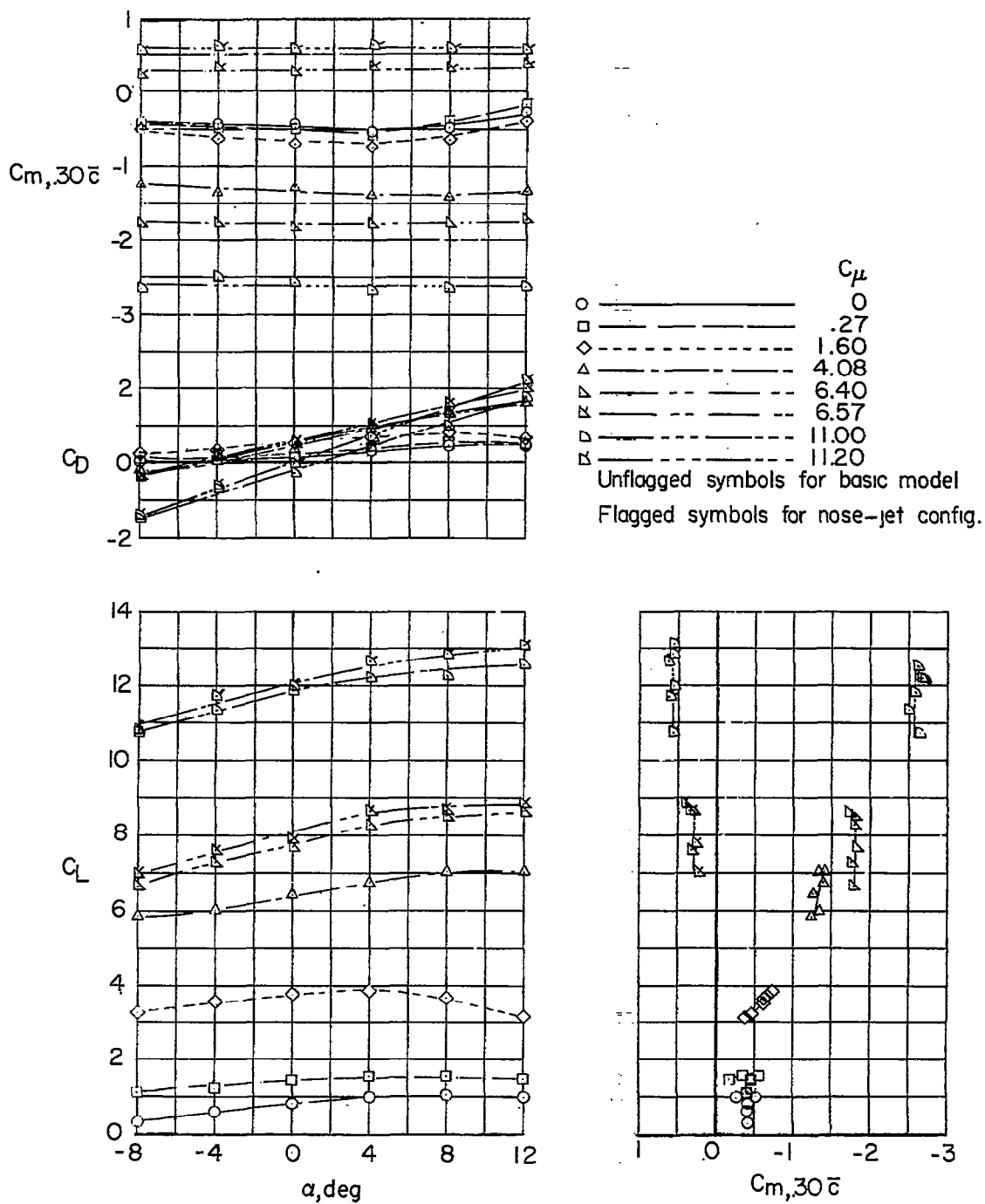


Figure 10.- Effect of nose jet on the static longitudinal stability and trim characteristics of the model in the landing condition.

$$\delta_f = 70^\circ; \delta_c = 0^\circ; i_t = 20^\circ.$$

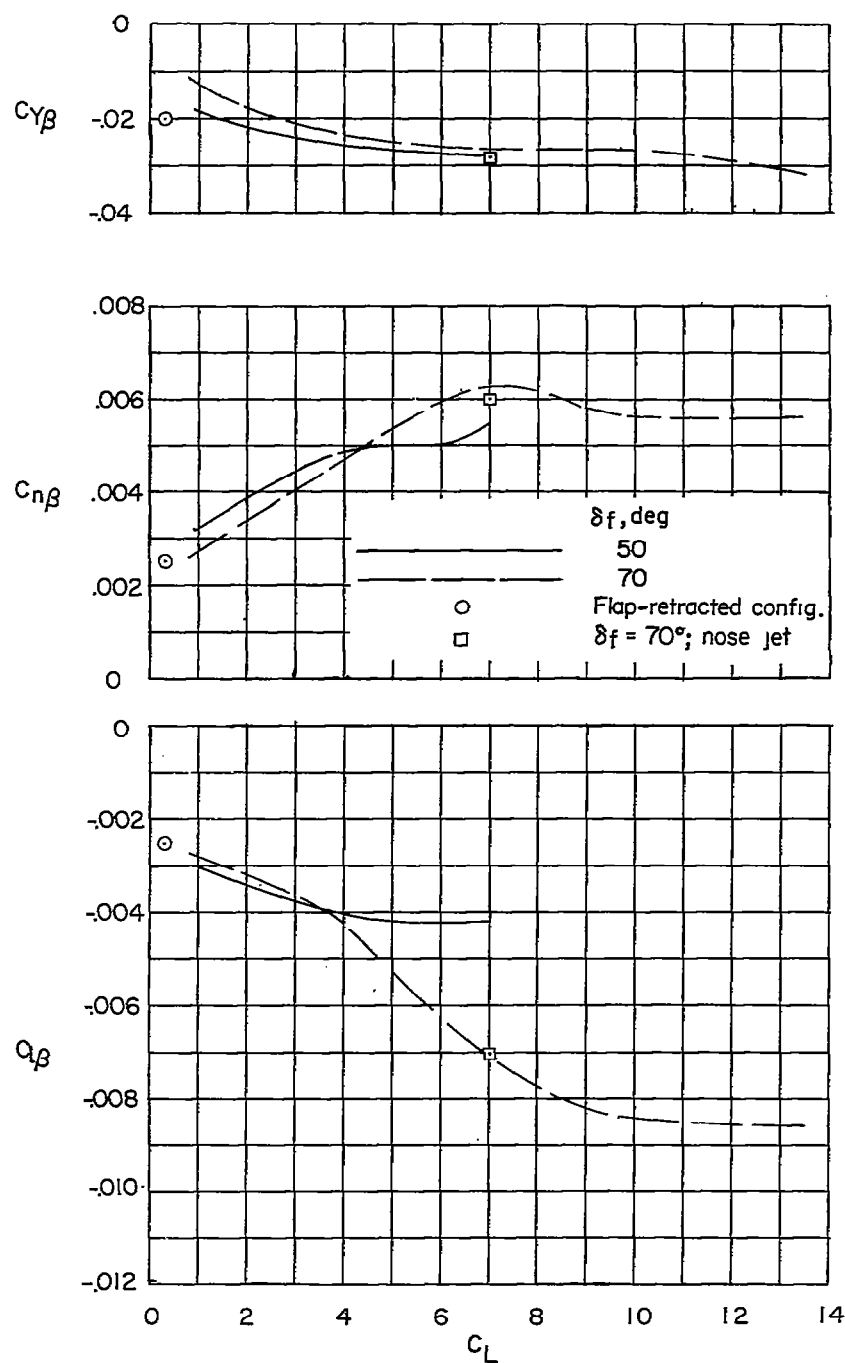
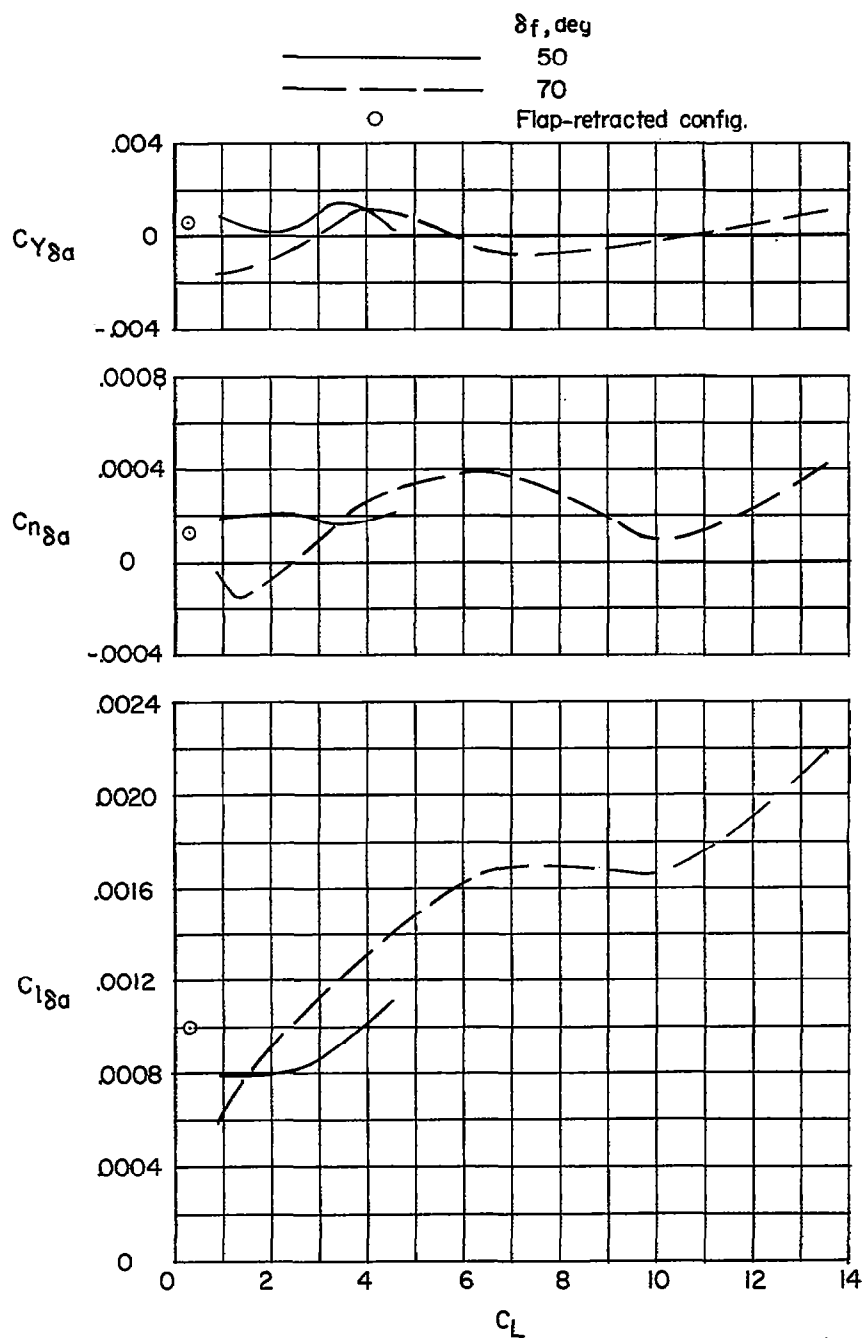
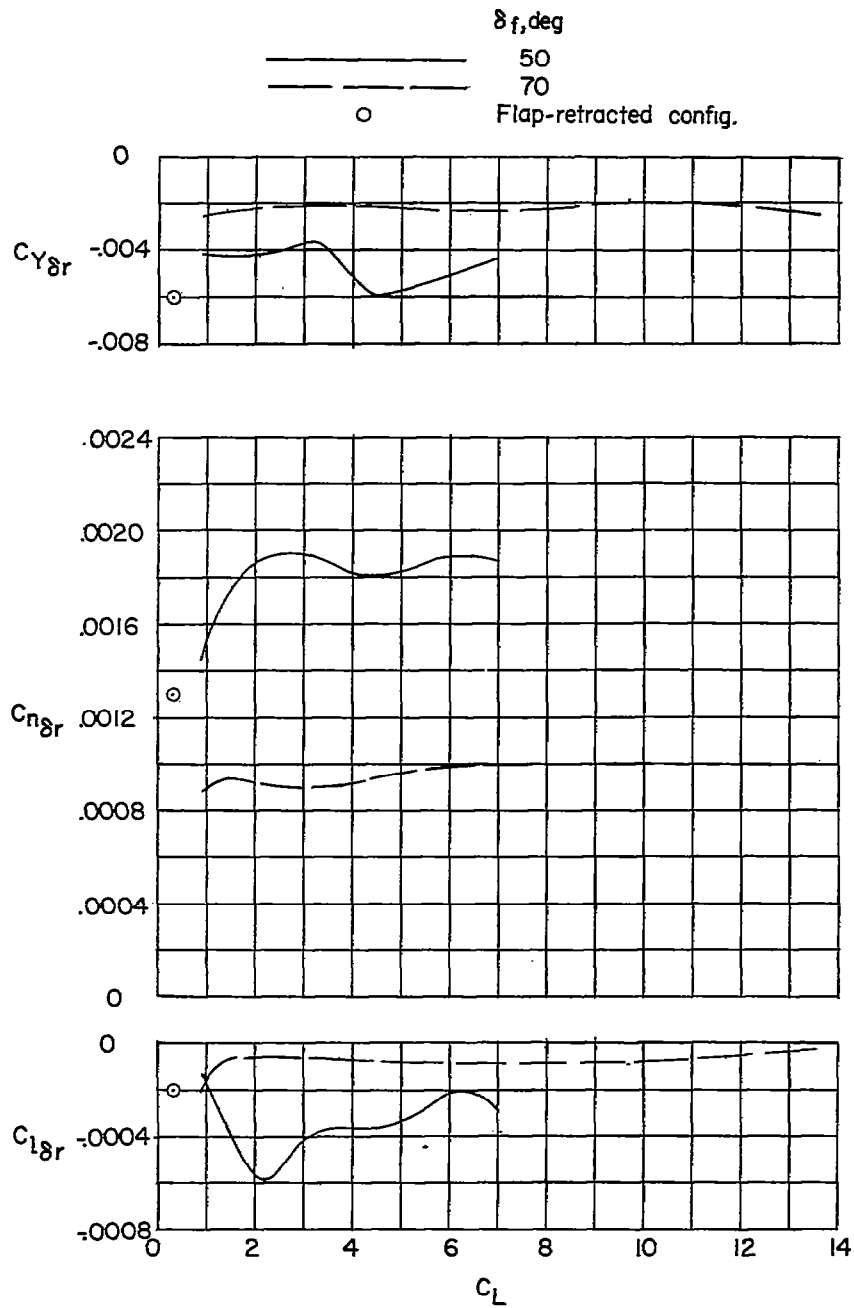


Figure 11.- Variation of the static-lateral-stability parameters with lift coefficient for flap deflections of 50° and 70° and for the flap-retracted configuration. $\alpha = 0^\circ$; $\beta = \pm 10^\circ$; $i_t = 20^\circ$.



(a) Aileron effectiveness.

Figure 12.- Variation of aileron- and rudder-effectiveness parameters with lift coefficient for flap deflections of 50° and 70° and for the flap-retracted configuration. $\alpha = 0^\circ$; $\beta = 0^\circ$; $i_t = 20^\circ$.



(b) Rudder effectiveness.

Figure 12.- Concluded.

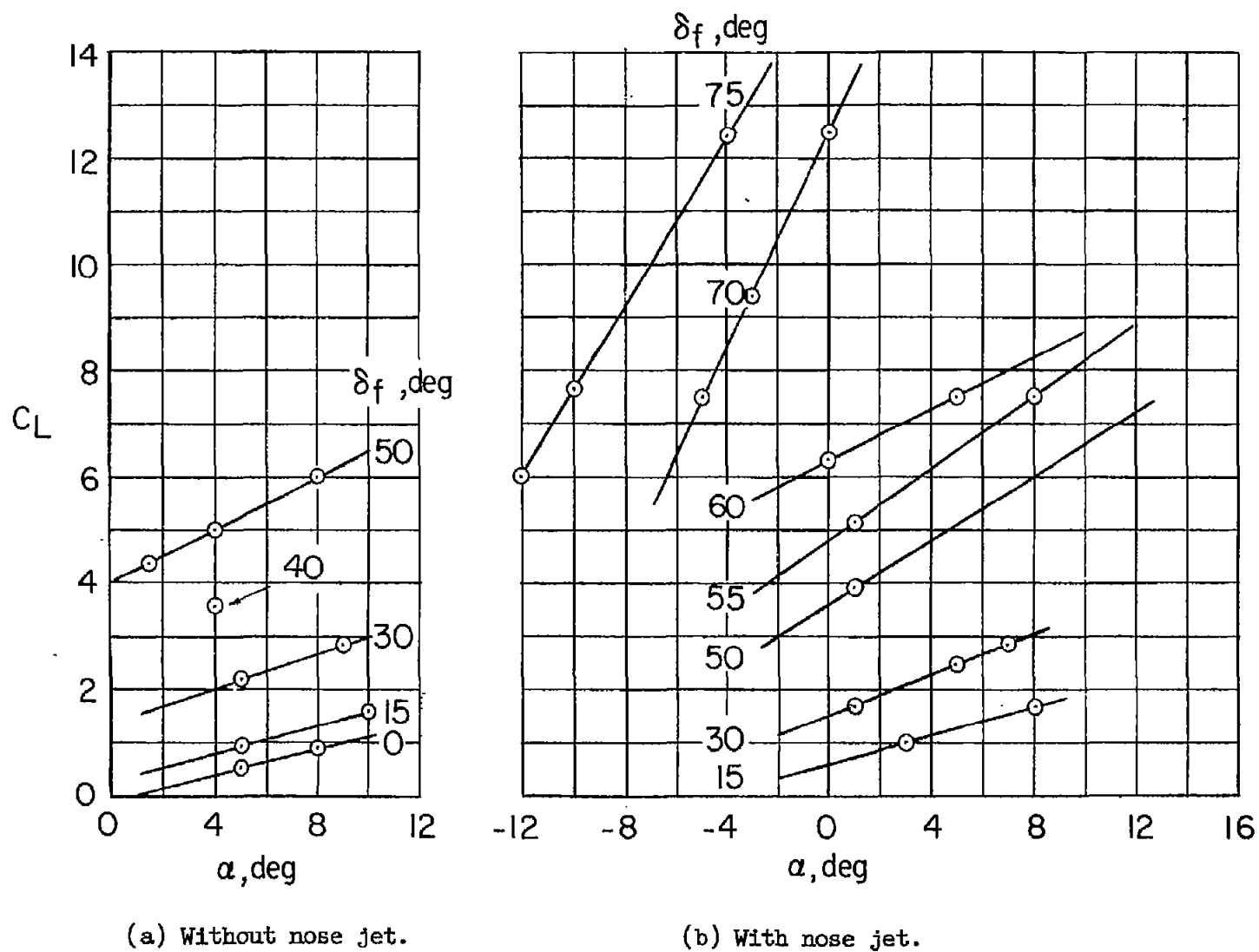


Figure 13.- Flight-test conditions of the investigation.

A motion-picture film supplement is available on loan. Requests will be filled in the order received. You will be notified of the approximate date scheduled.

The film (16 mm., 7 min., color, silent) deals with a wind-tunnel investigation at low speeds of the flight characteristics of a sweptback-wing jet-transport airplane model equipped with an external-flow jet-augmented slotted flap. The model was flown over a lift-coefficient range up to 12.5. For lift coefficients higher than about 6, a downwardly directed nose jet was used to supplement the trimming power of the horizontal tail.

Requests for the film should be addressed to the

Division of Research Information
National Advisory Committee for Aeronautics
1512 H Street, N. W.
Washington 25, D.C.

CUT

Date _____
Please send, on loan, copy of film supplement to TN 4255

Name of organization

Street number

City and State

Attention: Mr. _____

Title _____

Place
Stamp
Here

Chief, Division of Research Information
National Advisory Committee for Aeronautics
1512 H Street, N. W.
Washington 25, D. C